Advances in Aircraft and Spacecraft Science, *Vol. 5, No. 5 (2018) 595-613*
DOI: https://doi.org/10.12989/aas.2018.5.5.595

Damage of bonded, riveted and hybrid (bonded/riveted) joints, Experimental and numerical study using CZM and XFEM methods

M.C. Ezzine*[1], A. Amiri[1], M. Tarfaoui[2] and K. Madani[1]

[1]*Laboratoire Mécanique Physique des Matériaux (LMPM), Department of Mechanical Engineering, University of Sidi Bel Abbes, Sidi Bel Abbes 22000, Algeria*
[2]*ENSTA Bretagne, MSN/LBMS/DFMS, 2 Rue François Verny, 29806, Brest, CEDEX 9, France*

(Received January 30, 2018, Revised April 6, 2018, Accepted April 18, 2018)

Abstract. The objective of our study is to analyze the behavior of bonded, riveted and hybrid (bonded / riveted) steel / steel assemblies by tensile tests and to show the advantage of a hybrid assembly over other processes. the finite element method with the ABAQUS numerical code was used to model the fracture behavior of the different assemblies. Cohesive zone models (CZM) have been adopted to model crack propagation in bonded joints using a bilinear tensile separation law implemented in the ABAQUS finite element code. The riveted assemblies were modeled with the XFEM damage method identified in this ABAQUS numerical code. Both CZM and XFEM methods are combined to model hybrid assemblies. The results are consistent with the experimental results and make it possible to guarantee the validity of the applied numerical model. The use of a hybrid assembly shows a high resistance compared to other conventional methods, where the number of rivets has been highlighted. The use of the hybrid assembly improves mechanical strength and increases service life compared to a single lap joint and a riveted joint.

Keywords: single lap joint; riveted joint; hybrid joint; cohesive zone model (CZM); XFEM; steel E24

1. Introduction

The bonded assemblies are widely used in several engineering fields, such as automotive, aerospace and space structures, as an easy method to join components, ensuring at the same time design requirements for the structure (Lee *et al*. 2010). Bonded joints offer many advantages, in particular the assembly of different materials or composite materials (Adams 2005, da Silva 2008). The resistance of the assembly is directly related to the behavior of the adhesive since it has weak properties relative to those of the substrates. The analysis of the adhesive behavior was the primary concern of researchers. From the first work of Völkersen (1938), other models were developed on single or double lap joint (Adams 1974). The finite element method has been widely used to predict the behavior of bonded joints. Its greatest advantage is that it is very easy to modify the boundary conditions and geometries, to introduce non-linearities of behavior, to analyze structures made of different materials (Adams 1986) and thus to carry out complex parametric studies with a

*Corresponding author, Ph.D. Student, E-mail: ezzine_chamseddine@yahoo.fr

http://www.techno-press.org/?journal=aas&subpage=7 ISSN: 2287-528X (Print), 2287-5271 (Online)

three-dimensional modeling (Tsai 1993, 1995 and Apalak 2006).

The mechanical performance of adhesive-bonded steel joints has been studied in many research works using single lap-shear joint (Karachalios 2013a, Karachalios 2013b, da Silva 2009, Zhang 2013a, Zhang 2013b, De'Nève 1998), double lap-shear joint (Challita *et al*. 2011, Mokhtari *et al*. 2013), coach-peel joint (Challita 2011), wedge-peel joint (Blackman 2000), butt joint (Seo 2005), and component test (Peroni 2009, Lee 2006). Karachalios performed single lap-shear tests with high-strength steels and low carbon steels, and even for composite metal joints (Russo 2013).

To take full advantage of the benefits of bonding over mechanical fastening, considerable research has been done over the past several decades in bonding of aluminum (Rezgani *et al*. 2016, Elhannani *et al*. 2017). A detailed study of adhesive bonded metallic structures is reported in the Primary Adhesively Bonded Structure Technology (PABST) Program (Thrall 1977, 1979). Earlier studies on adhesive-bonded joints can be found from the review papers by Matthews *et al.* (1982) and Vinson (1989). Hart-Smith (1973) and Lees (1985) included elastoplastic adhesive behaviour. All these theoretical studies neglected adherent shear deformations and did not provide detailed stress concentrations at critical regions. Although more refined theories, including nonlinear geometric and material effects of the adhesive and adherents have been presented (Tsai and Morton 1994, Harris and Adams 1984). The finite element method is widely used in the technology and its application to the determination of stresses in structures assembled by adhesive has a great advantage (Benchiha *et al*. 2016, Elhannani *et al*. 2016) Wooley and Carver (1971) made one of the first finite element analysis of an assembly single lap.

The riveted joints are often used in aerospace, railway structures and automotive. Mechanical fasteners such as rivets were commonly used in the aerospace industry for several decades (Matthews *et al.* 1982 and Vinson 1989). This technique provides an assembly of good electrical conductivity and the ease of disassembly of the components. The major problem that arises in a riveted joint is the high stress concentrations around the fixing holes which increases the risk of failure of the structure, including the locating of these cracks is only possible once their size exceeded the rivet head. This assembly technique is used to join metals of the same or different natures (aluminum, steel) (Al-Bahkali 2011) and even the composites (Ireman *et al*. 1993), with rivets made of aluminum alloy, steel etc. Several research studies have been done to study the mechanical behavior of the riveted structures by analytical, and experimental approaches, or numerical simulations (Collings 1977, Reid and Hiser 2005).

However, the latest research aims to combine the two types of joints and improve the individual performance of each type of joint. Modern applications of hybrid joints (bonded + riveted (Gomez *et al*. 2007), bonded + bolted (Kelly 2006)) are of great technological interest. This technique is of great importance in engineering such as aerospace. A number of experimental studies have shown that these assemblies can potentially achieve high static resistance than bonded, riveted or bolted joint separately (Hart-Smith 1985, Chan 2001, Fu and Mallick 2001, Kweon *et al.* 2006). Compared to a riveted structure, it reduces the number rivets and improve the aesthetics and strength of the structure.

However, the majority of the latest work is focused on the study of this type of process (hybrid), which is the context of our work where our objective is to study by tensile tests the mechanical behavior of an assembly of steel / steel type by different processes: bonded, riveted and hybrid.

The use of a hybrid assembly improves the strength of the assembly by minimizing the number of rivets in the structure. Energy Absorption (EA) for different joints has been studied, where it has been shown that the hybrid joint requires more energy compared to a bonded or riveted one.

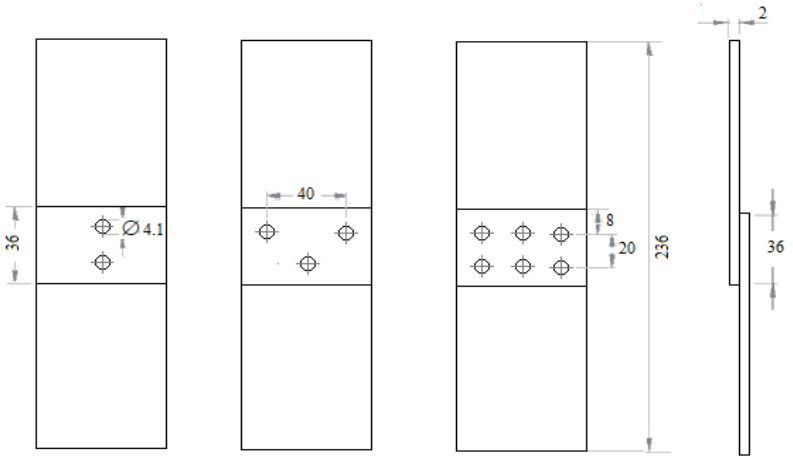

Fig. 1 Geometric model of riveted joints, case 2 rivets, 3 rivets and 6 rivets

Table 1 Mechanical properties of the rivet

Properties	Values
Young's modulus [GPa]	70
Tensile strength [MPa]	135
Yield strength [MPa]	60
Shear modulus [Gpa]	26.51
Poisson's ratio	0.33

Finite element numerical modeling with the ABAQUS numerical code has been used to simulate the fracture behavior of bonded, riveted and hybrid assemblies. Cohesive zone models (CZM) using a bilinear traction-separation law and an XFEM model were adopted to model the damage of the joints tested.

2. Experimental procedure

In order to study the performances of the different types of assembly, two E24 type steel plates were assembled by different processes (bonding, riveting and hybrid) and subjected to a uniaxial tensile load.

For riveted joints, the number of rivets varies for each case of assembly (2, 3 and 6 rivets) (Figure 1). The rivets have a diameter of 4mm (Figure 2). The riveting of the two plates is done using a manual riveter. The distance between the rivets and the edge of the plate is standardized and is between 1.5d and 2.5d. The distance between the rivets is equal to 5d. The rivets are of aluminum alloy and are shown in (figure. 2b) (Sadowski *et al.* 2010).

The mechanical properties of the plates, rivets and adhesives are presented in Table 1, 2 and 3. These mechanical properties were derived from the tensile curves made on samples of each component used in the assembled structure see Figures 2 and 3. Only the properties of the two steel plates were taken directly from the literature (reference).

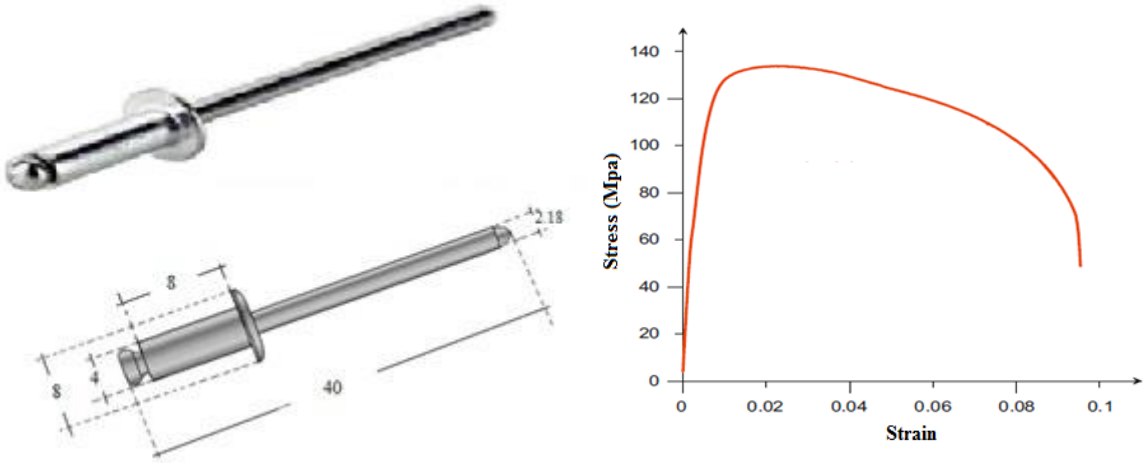

(a) Dimension of rivet (b) Stress-strain curve for aluminum rivet

Fig. 2 Dimension and stress-strain curve of aluminium rivet

Table 2 Mechanical properties of steel E24 plate

Properties	Values
Young's modulus [GPa]	205
Tensile strength [GPa]	11.1
Yield strength [GPa]	7.1
Schear modulus [Gpa]	80
Poisson's ratio	0.32

Table 3 Mechanical Properties of the Adhesive 'Adekit A140'

Properties	Values
Young's modulus[MPa]	2660
Tensile strength[MPa]	22.7
Yield strength[MPa]	7.02
Elongation at failure [mm]	0.032
Poisson's ratio	0.35

For the bonded process, the two steel plates are assembled by an epoxy adhesive of type Adekit A140 marketed by AXON (France) (Figure 3). This adhesive is widely used in different fields because of these important mechanical characteristics with respect to the mechanical and thermal stresses. This adhesive is in the form of a two-component tube. This adhesive has an excellent mechanical and thermal performance up to 100°C and excellent resistance to dynamic loads (vibrations and impacts) and is a product resistant to aging and aggressive environments (Rezgani *et al*. 2018).

Tensile tests were performed on the adhesive bulk to determine these mechanical characteristics that will be introduced into the numerical model (Table 1).

The preparation of the surfaces of the two plates plays an important role to have a good

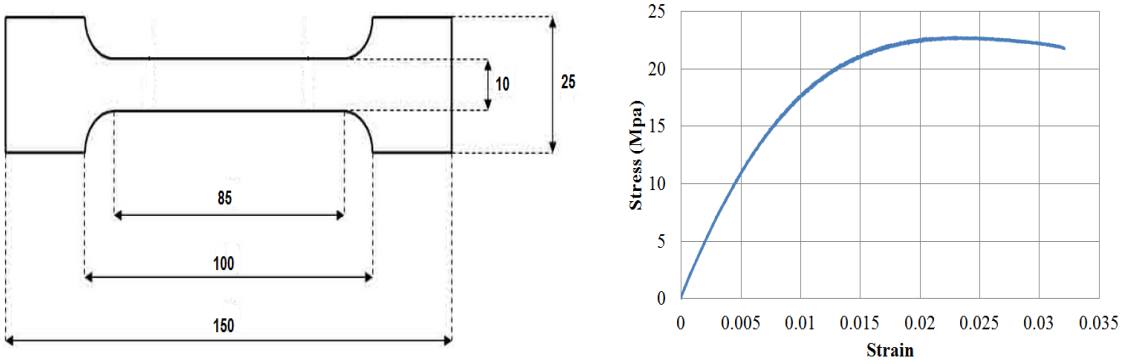

(a) Geometry of the specimen (b) Stress-strain curves for ‘Adekit A140’

Fig. 3 Stress-strain curve for Adekit A140

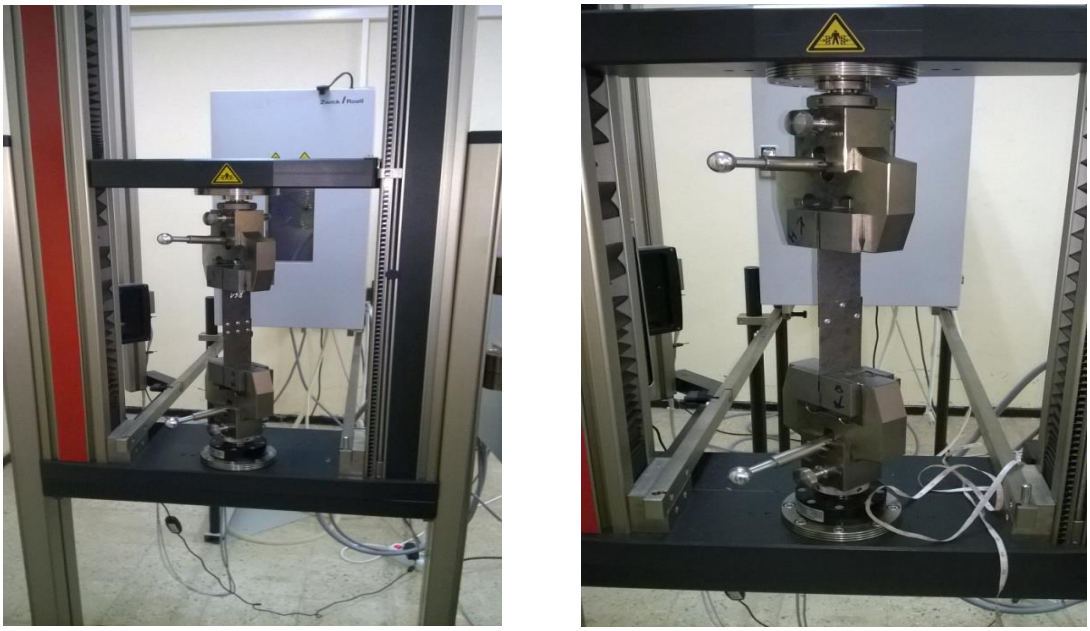

(a) Riveted joint with 6 rivets (b) Stress-strain curves for ‘Adekit A140’

Fig. 4 Tensile tests of the riveted and hybrid joints

adhesion, for this, the plates were sandblasted with fine grain and brazing with a medium speed and chemical treatment using acetone to have a surface ready to stick and clean any dust. The bonding surface is 36x56 mm with a thickness of 0.2 mm adhesive.

The third joint tested is the hybrid joint, this joint combines the two types of assembly mentioned above keeping the same dimensions for the two plates, the rivets and the adhesive. The adhesive was applied to the facets of the cleaned steel plates and then the joint was reinforced with rivets.

Samples containing adhesive were tested at least 3 days after their preparation so that the adhesive crosslinks under good conditions.

The specimens were subjected to tension load, using the testing machine of Zwick Roell a

Fig. 5 Results of tensile tests in steel plates for different types of joints

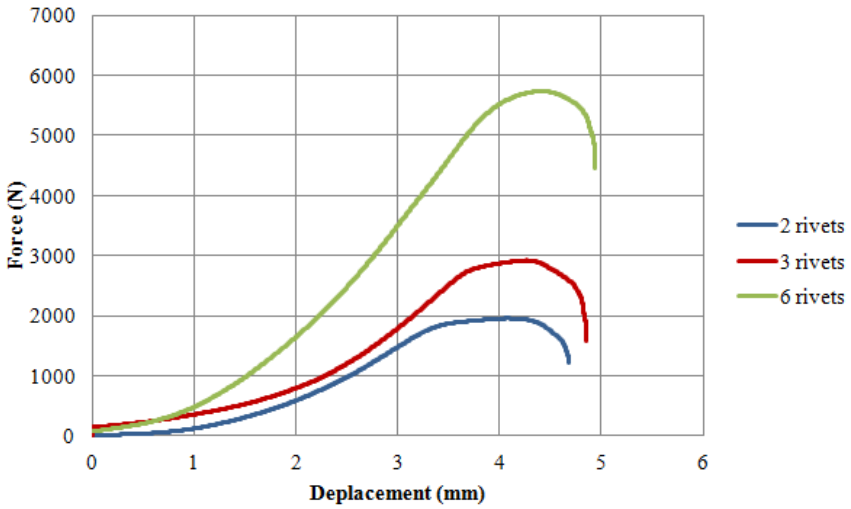

Fig. 6 Force-displacement curves for riveted joints

crosshead displacement rate of 0.5 mm / min (Figure 4). The uniaxial tensile tests for the different joints were carried out under the same conditions.

Figure 5 shows the results of the different assemblies after fracture. It can be noted that the rivet deforms significantly in shear and where the steel plates are slightly deformed at the edge of the holes. The maximum deformation in the rivet occurs in its central part which corresponds to the central region of the connection.

In order to have satisfactory results of the tensile tests on the different assemblies, at least three samples of each assembly were tested; sometimes we had a slip in the jaws of the machine so we had to add more samples. The experimental results of the tensile test for the different types of assembly are shown in Figures 6 and 7.

The analysis of the results of the different tensile tests is presented as a force-displacement curve for the various configurations.

The first attempt was to group the results of the assembled samples by rivets alone, and those with separate adhesive (Figures 6 and 7).

Note for the various riveted joints (Figure 6) that the mechanical behavior is almost similar to the beginning of loading, a significant displacement in front of a low load. On the other hand, if one exceeds a certain load which differs from one configuration to another, the slope of the curve

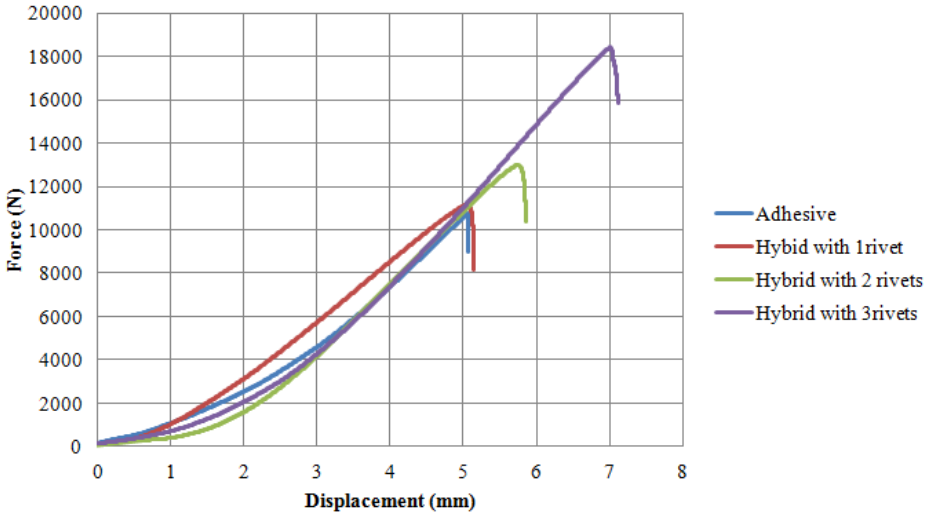

Fig. 7 Force-displacement curves for bonded and hybrid joints

increases sharply. The steel parts joined by the rivet have a relatively low resistance. This is because the rivet was aluminum alloy, not having a high shear strength limit. The more the number of rivets increases, the structure is more resistant to the applied load and the slope of the curve is more and more acute. The applied force will be transmitted directly to the rivets, a plasticization of the latter is noted before it shears completely.

On the other hand, the bonded plates with Adekit A 140 were extremely effective and hard, that is, the joint strength is almost an order of magnitude higher than the riveted joints (Figure 7). The shape of the force-displacement curve is characteristic that is to say after the first linear part, the curve reaches the local maximum where the adhesive layers begin to be damaged.

The same behavior is noted for the hybrid assembly as for the bonded assembly (figure 7), to which the adhesive layers begin to fail in the first step, a linear behavior, then the yield of the steel strips and finally the crack propagation in the adhesive layers (after maximum load) in the most strained area of the joint. However, an increase in the failure load can be observed due to the presence of the rivets. In addition, a significant increase in displacement at failure is observed for hybrid joints. Damage occurred on both interfaces and rivets, the fracture surface is presented in Figure 5.

In the force-displacement tensile curves, the values of forces and displacements are much higher in the case of the hybrid assembly. The change of the slope of the curve differs from one configuration to another. The joint with only adhesive has a high resistance compared to riveted joints but also a low value compared to hybrid joints. The applied force will be transmitted at the same time to the adhesive and the rivet and a small part to the plate.

The increase in the number of rivets improves the mechanical strength of the joint and minimizes the concentration of stresses at the different rivets. By using a hybrid joint, the number of rivets in an assembled riveting structure can be clearly reduced and the stress concentration avoided.

Figures 8 and 9 are plotted to see more clearly about the behavior of different configurations, where the maximum values of force and displacement are grouped in histograms forms.

It is clear that the maximum force in a riveted joint increases from 2000N for the case of two

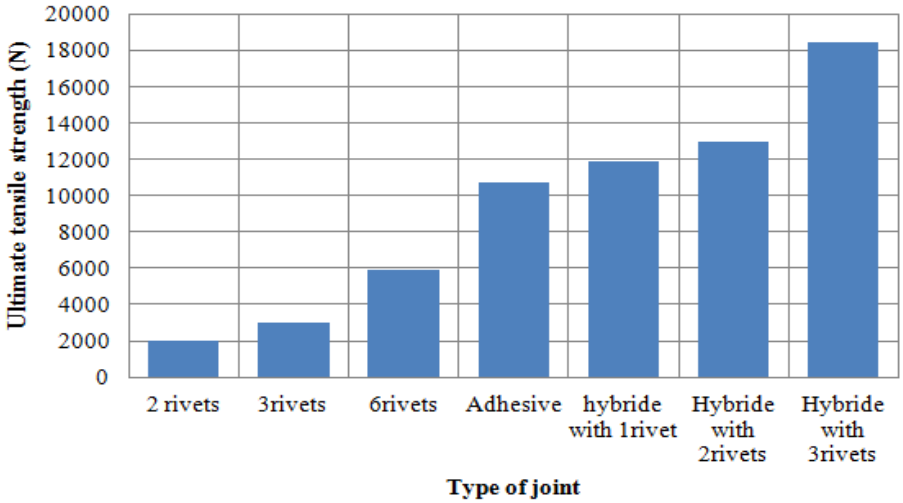

Fig. 8 Maximum force for each type of assembly

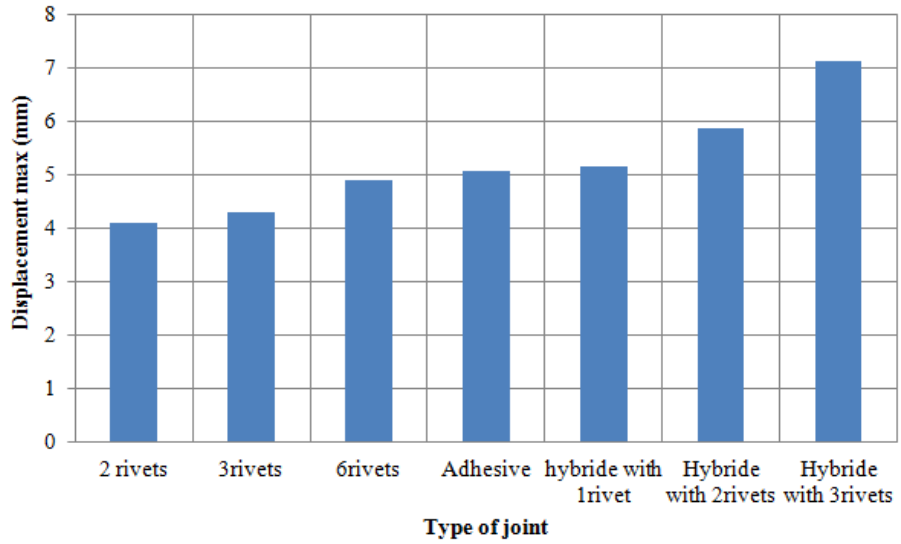

Fig. 9 Maximum displacement value for each type of assembly

rivets to 6000N for the case of 6 rivets. The increase in the number of rivets generates the creation of the stress concentration on the one hand and additional weight on the other hand. Increasing the number of rivets in the overlap area may cause damage to the plate, since the rivet hole may be near the free edge of the plate. On the other hand, the presence of the adhesive increases the strength of the assembly by more than twice than for the riveted assembly (6 rivets) and six times for the case of 2 rivets.

For the hybrid assembly (with 1 rivet), the behavior is almost similar to the joint with only adhesive and at almost the same value of the maximum force. The hybrid configuration (with 3 rivets) is significantly better than for the other configurations, the value of the force increases by more than nine times than for the assembly with two rivets and three times that for the assembly

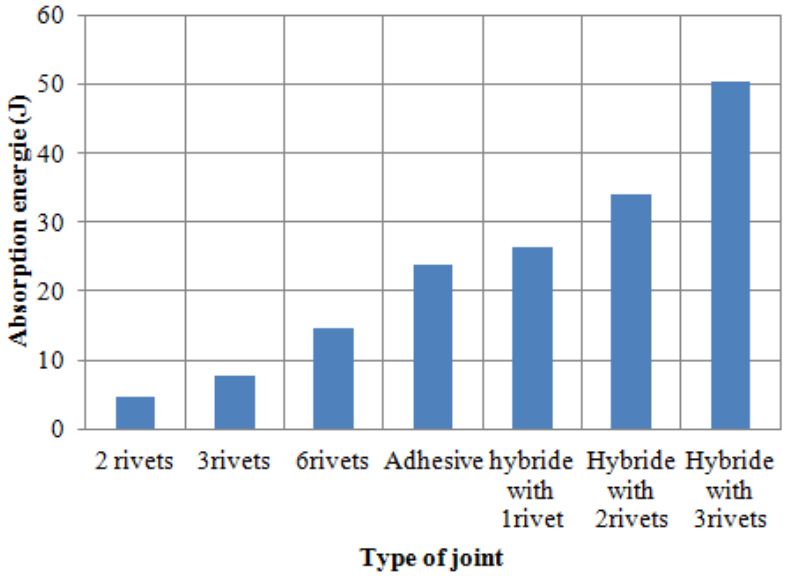

Fig. 10 Variation of energy absorption for the different joints

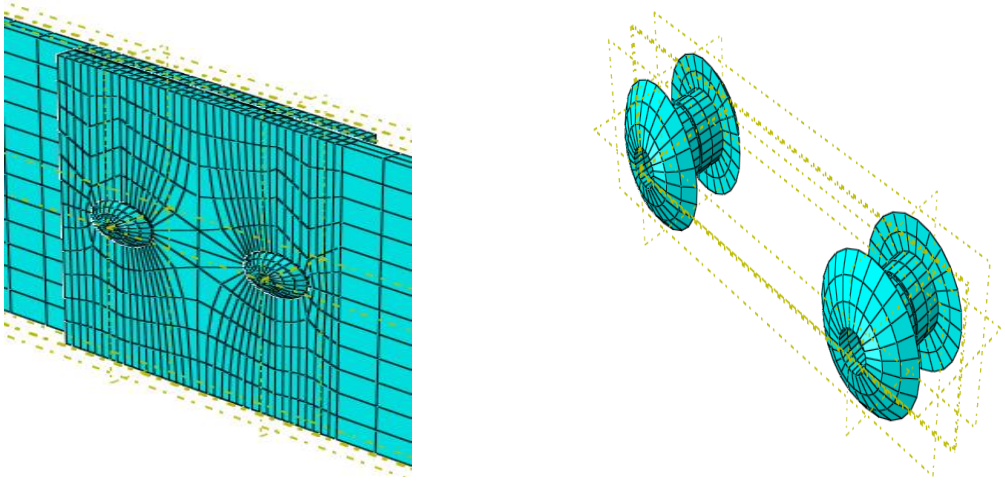

(a) (b)

Fig. 11 Mesh of a) riveted joint and b) rivets

with six rivets and almost twice that for a bonded assembly.

For the value of the maximum displacement in the different joints (Figure 9), it is clear that the displacement value is almost identical for riveted configurations regardless of the rivet number. Hybrid joints have significantly higher displacement values than adhesive and only rivets.

From the perspective of weight of joints, a single riveted joint with 6 rivets has the same weight as a hybrid joint with 1 rivet. So we can reduce the number of rivets in a joint and replaced by an adhesive layer keeping the same weight with better performance and eliminating the disadvantages of each type of assembly (bonded and riveted).

Table 4 The mechanical properties of the adhesive 'ADEKIT A140' and cohesive model

E (MPa)	ν	G_{Ic} (KJ/m²)	G_{IIc} (KJ/m²)	T_n (MPa)	T_s (MPa)
2660	0.35	0.5	2.41	35.9	30.9

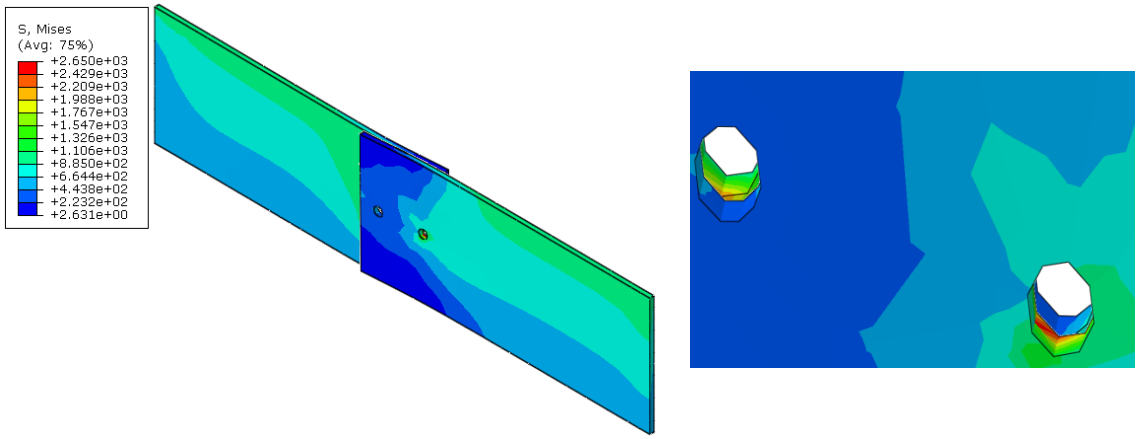

(a) stress in the plates

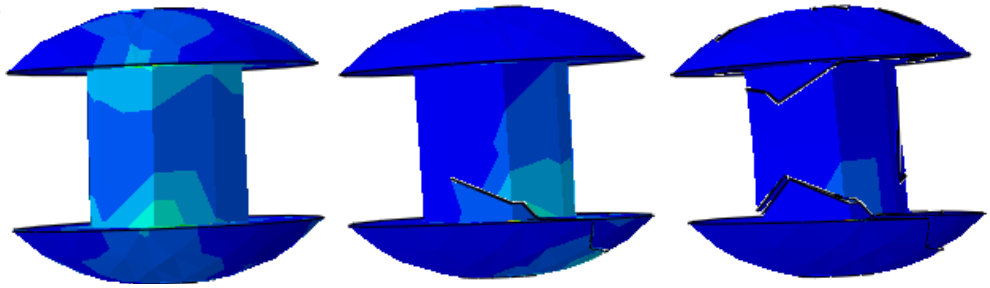

(b) the shearing sequence of the rivet

Fig. 12 Damage of the riveted joint during tensile loading

3. The energy absorption

The energy absorption (EA) was calculated from the areas of the experimental tensile test curve surfaces for each configurations. A comparison of EA for the considered types of joints was presented in Figure 10. This comparison leads to the conclusion that most of the strength of the hybrid joints comes from the adhesive. However, the addition of rivets significantly increases the energy absorption capacity of hybrid joints. The increase in the number of the rivet improves the value of the energy, and an increase of almost 69% was noted for the case of the assembly with 3 rivets compared to a single rivet. In the case of the hybrid joint with 3 rivets, this increase was equal to 90% compared with a riveted joint with a rivet and 50% with a bonded joint.

4. Numerical study

A three dimensional (3-D) finite element model was established in order to investigate

numerically the behaviour of different types of joint. The following types of elements were applied to the analysis: 8-node brick elements with reduced integration for modelling the steel adherends response, 4 node tetrahedral elements were used for the rivet modelling and 8-node three-dimensional cohesive elements for the adhesive layer. The analyses were done with the explicit version of the ABAQUS finite element code using arbitrary Lagrangian–Eulerian adaptive meshing. The parameters used in the cohesive models (G_{Ic}, G_{IIc}, Tn, Ts) for the adhesive were determined following tests of DCB and ENF carried out in the laboratory (Table 4).

4.1. FEM model of the riveted joint

Figure 11 shows the mesh of the components of the riveted joint (the adherents and the rivet). In order to model the contact between the adherents and the rivet, ABAQUS / Explicit's general contact algorithm was used with edge-to-edge contact penetrations. The contact properties were considered a "hard" contact in the normal direction without friction.

Figure 12 shows the sequence of events during uniaxial loading of the riveted joint. The stress concentrations in the rivet appear in the shear planes. Rivets made of Aluminum are modeled by the XFEM method included in the numerical code 'Abaqus'. When the maximum shear resistance of the rivet is reached at any point of the rivet, finally, the rivet is damaged.

The results obtained numerically for riveted joints are presented in the form of force-displacement curves (Figure 13). These numerical curves are compared with the experimental results, where the numerical and experimental curves are combined.

The sliding of the mores during the experimental tests is visible in the curves, where this effect does not exist in the numerical curves. For this we see a shift in the axis of displacement. The numerical curves show consistent results to experimental tests.

4.2. FEM model of adhesive joint

In order to simulate gradual decohesion and the failure process of the adhesive layer, a CZM model was applied in FEA calculations.

4.2.1. Cohesive zone model

A cohesive zone model is used to analyse the propagation of cracks. The cohesive zone is defined as a row of cohesive elements where the crack growth will occur. The cohesive law chosen to model the behaviour of the adhesive interfaces/substrate is a bilinear traction-separation law (TSB) proposed by Camanho (2002), implemented in the finite element code ABAQUS.

The tensile or shear stress (T_i, i = n; t) at the interface increases linearly with the opening δ_i, at a slope described by the parameter K representing the initial stiffness of the cohesive zone.

When the critical stress $T_{i,\max}$ is reached, the interface begins to damage. Finally, the opening between the two lips of the interface reaches a critical value $\delta_{i,m}$ corresponding to the rupture of the interface (Fig. 14).

The relationship Traction-separation can be expressed as:

$$T_i = \begin{cases} (1-D)K\delta_i, \\ D = \dfrac{\delta_{i,m}}{\delta_{i,m}-\delta_{i,0}} \left(1-\dfrac{\delta_{i,0}}{\delta_i}\right) \text{ if } \delta_i > \delta_{i,0} \text{ if not } D = 0 \\ D = \min(D, 1) \end{cases} \tag{1}$$

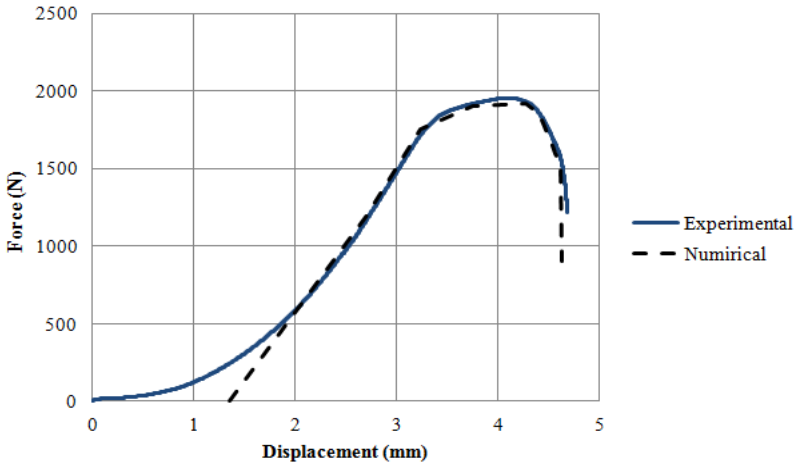

(a) with 2 rivets

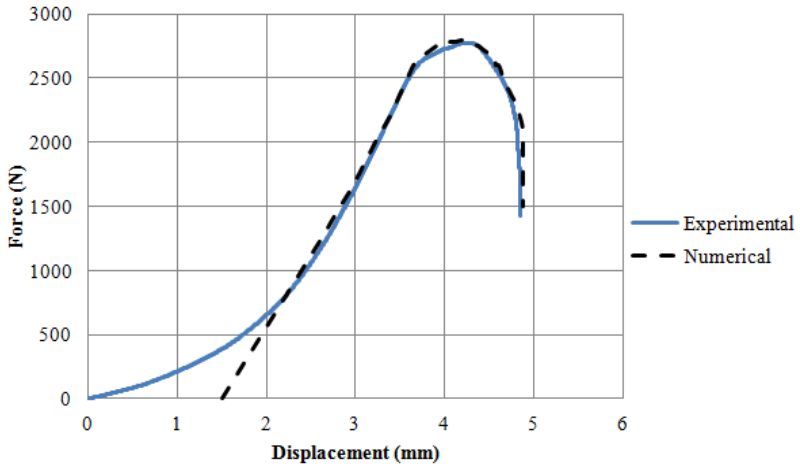

(b) with 3 rivets

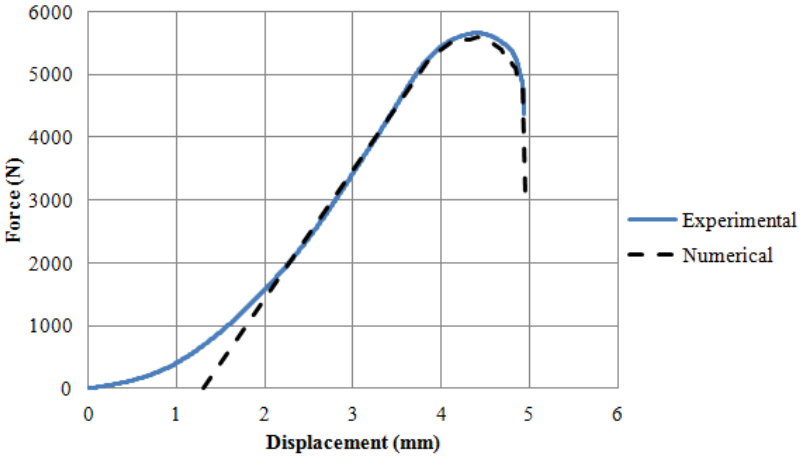

(c) with 6 rivets

Fig. 13 Numerical and experimental load-displacement curves of the riveted joint

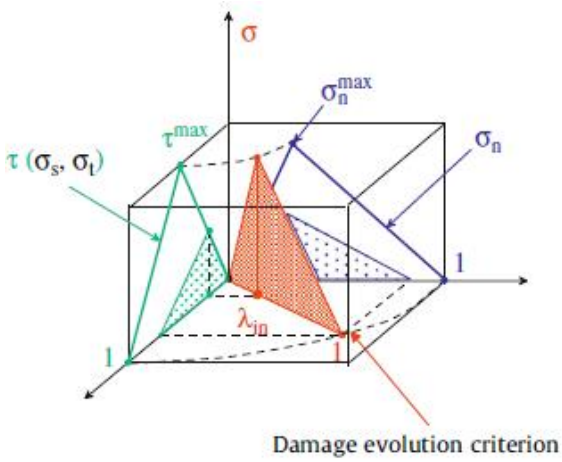

Fig.14 Bilinear traction-separation Law

D is a damage variable. The critical stress $\mathbf{T_{i,\,max}}$, critical opening $\boldsymbol{\delta_{i,m}}$ and energy release rate $\mathbf{G_{ic}}$ are linked by the following formula:

$$G_{ic} = \frac{T_{i,max} \text{ x } \delta_{i,m}}{2} \tag{2}$$

Under each of the failure modes (pure mode I or pure Mode II), the law for describing the behaviour of the interface with two physical parameters among $\mathbf{T_{n,max}}$, $\mathbf{G_{Ic}}$ and $\boldsymbol{\delta_{n,m}}$ mode I, and $\mathbf{T_{t,max}}$, $\mathbf{G_{II,c}}$ et $\boldsymbol{\delta_{t,m}}$ mode II (Fig. 14).

To model the behaviour of an interface in a mixed load, it is necessary to:

- Identify the parameters in each pure mode (I and II)
- Define a criterion of initiation of damage
- Define a failure criterion.

4.2.2. Criterion for initiation of damage

A quadratic stress criterion (QUADS DAMAGE) has been adapted to characterize the initiation of the damage. It involves both the critical tensile stress Tn, max and the critical shear stress Ts, max, (Campilho *et al*. 2009):

$$\left\{\frac{\langle t_n \rangle}{T_{n,max}}\right\}^2 + \left\{\frac{t_s}{T_{s,max}}\right\}^2 = 1 \tag{3}$$

< >, Macaulay brackets indicate that only the normal traction may initiate damage.

4.2.3. Criterion of damage propagation

A criterion of propagation of damage (Power Law) was used, it allows us to define the crack propagation in mode I, Mode II and mixed mode I / II. It will be based on the energy release rate G:

$$\left[\frac{G_I}{G_{IC}}\right]^{\alpha} + \left[\frac{G_{II}}{G_{IIC}}\right]^{\alpha} = 1 \tag{4}$$

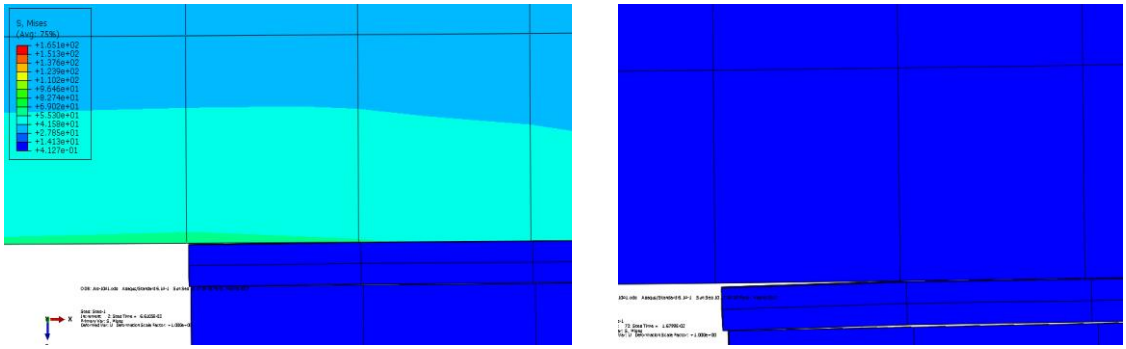

(a) Initial failure (b) Final failure

Fig. 15 Progressive damage in the adhesive joint

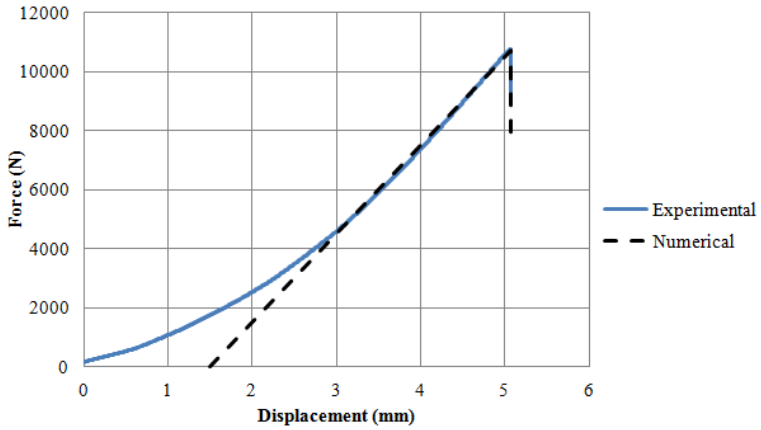

Fig. 16 Numerical and experimental load–displacement curves of the adhesive joint

4.3.4. Mixed Loading

Under a mixed load between the normal and tangential directions, define an equivalent effective displacement and a corresponding effective stress dependent normal value and tangential, as follows:

$$T_{eq} = \sqrt{T_n^2 + T_t^2} \ , \ \delta_{eq} = \sqrt{\langle \delta_n \rangle^2 + \delta_t^2} \tag{5}$$

Calibration process parameters of the cohesive law, coupling experimental and modelling is then proposed from identification tests in each pure mode and validated on an adhesion test by simultaneously involving both stress modes cited in Table 3.

4.3.5. Initial stiffness of the cohesive zone K

To avoid numerical instability problems and generally generates no convergence of computing, a cohesive model with a sufficiently high initial stiffness seems a most suitable solution.

$$K = \beta \frac{E}{h} \tag{6}$$

where E is Young's modulus of the adhesive and h the thickness of the adhesive layer.

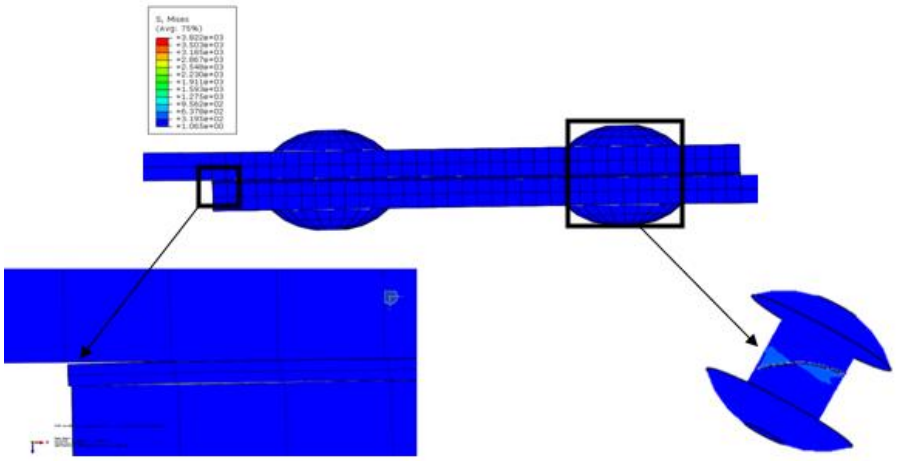

Fig. 17 Damage of the adhesive and the rivet in hybrid joint

Damage to the bonded assembly is shown in the Figure 15, in which stress concentration is observed from the beginning of the tensile deformation process at the edges of the adhesive.

Due to the concentration of stresses at the ends of the adhesive layer, the damage initiation criterion is satisfied and the degradation process starts from the adhesive edges. The central portions of the adhesive layers are subjected to a low stress level and do not support a significant amount of the load. Figure 15(b) shows the final failure phase.

Figure 16 shows the force-displacement curve that compares experimental results and numerical calculations. Numerical modeling with the hypotheses presented above compares well with the experiments, although in the final phase.

4.4. FEM model of the hybrid joint

A comparison of experimental results and numerical simulation for the hybrid joint is shown in Figure 18. The shape of the force-displacement curve is similar to the purely adhesive joint, but the failure load has been increased by the rivet. The process of progressive degradation starts in the adhesive layers, while, the total capacity of the adhesive layers is reached and the shearing of the rivet will take place. It must be emphasized that, in all the types of joints analyzed, the level of stresses in the steel members does not exceed the elastic limit.

5. Conclusion

In this work, riveted, bonded and hybrid joints (adhesive and rivets) have been studied experimentally and numerically. Numerical analysis, with the application of a cohesive zone model and the XFEM method, was practiced for the description of adhesive, riveted and hybrid joints.

The numerical results compare well with the experimental data. The results obtained in the paper lead to the following main conclusions:

- Increasing the number of rivets in a single riveted joint meeting the assembly standards gives more resistance to the joint it means that efforts are shared in all rivets.

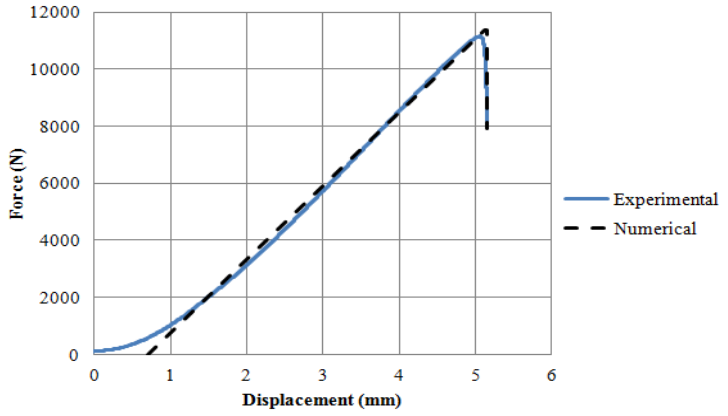

(a) with 1 rivets

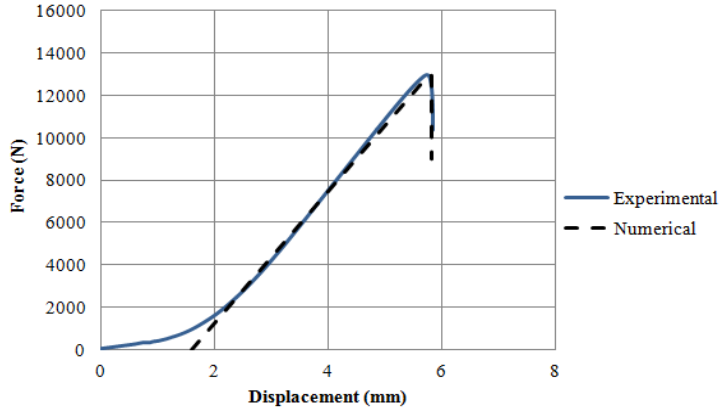

(b) with 2 rivets

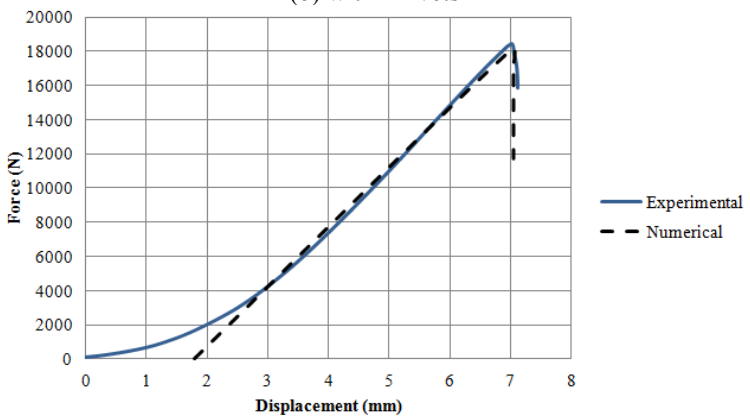

(c) with 3 rivets

Fig. 18 Numerical and experimental load-displacement curves of the hybrid joint

- A single lap adhesive joint with 'Adekit A140' with good surface treatment of the substrates, gives good strength and higher absorption energy than a riveted gasket with 6 rivets.
- The reinforcement of the adhesive joints with single overlap by rivets gives the joint a

higher resistance.

- The numerical results validate and confirm the results obtained experimentally on the different joints.
- Hybrid assemblies lead to greater reliability and durability of the structural assembly of different parts such as: automotive, nautical, aerospace and other engineering branches.

References

Adams, R., Atkins, R., Harris, J. and Kinloch, A. (1986), "Stress analysis and failure properties of carbon-fibre reinforced plastic/steel double lap-joint", *J. Adhesion*, **20**(1), 29-53.

Adams, R.D. (2005), *Adhesive Bonding: Science*, *Technology and Applications*, Woodhead Publishing Ltd., Bristol, United Kingdom.

Adams, R.D. and Peppiatt, N.A. (1974), "Stress analysis of adhesive-bonded lap joints", *J. Strain Analysis*, **9**(3), 185-196.

Al-Bahkali, E.A. (2011), "Finite element modeling for thermal stresses developed in riveted and rivet-bonded joints", *J. Eng. Technol.*, **11**(06), 86-92.

Apalak, Z., Apalak, M. and Genc, M. (2006), "Progressive damage modeling of an adhesively bonded unidirectional composite single-lap joint in tension at the mesoscale level", *J. Thermoplastic Compos. Mater.*, **19**(6), 671-702.

Benchiha, A., Madani, K., Touzain, S. and Ratwani, M. (2016), "Numerical analysis of the Influence of the presence of disbond region in adhesive layer on the stress intensity factors (SIF) and crack opening displacement (COD) in plates repaired with a composite patch", *Steel Compos. Struct.*, **20**(4), 951-962.

Blackman, B.R.K., Kinloch, A.J., Taylor, A.C. and Wang, Y. (2000), "The impact wedge-peel performance of structural adhesives", *J. Mater. Sci.*, **35**(8), 1867-1884.

Camanho, P.P. and Davila, C.G. (2002), "Mixed-mode decohesion finite elements for the simulation of delamination in composite materials", NASA/TM-2002-211737; NASA Langley Research Center, U.S.A.

Campilho, R.D.S.G., de Moura, M.F.S.F., Ramantani, D.A., Morais, J.J.L. and Domingues, J.J.M.S. (2009), "Buckling behaviour of carbon–epoxy adhesively-bonded scarf repairs", *J. Adhes. Sci. Technol.*, **23**(10-11),1493-1513.

Challita, G., Othman, R., Casari, P. and Khalil, K. (2011), "Experimental investigation of the shear dynamic behavior of double-lap adhesively bonded joints on a wide range of strain rates", *J. Adhes. Adhes.*, **31**(3), 146-153.

Chan, W.S. and Vedhagiri, S. (2001), "Analysis of composite bonded/bolted joints used in repairing", *Compos. Mater.*, **35**(12), 1045-1061.

Collings, T.A. (1977), "The strength of bolted joints in multi-directional CFRP laminates", *Composites*, **8**(1), 43-55.

da Silva, L.F.M. and Öchsner, A. (2008), *Modeling of Adhesive Bonded Joints*., Springer, Berlin, Germany.

da Silva, L.F.M., Carbas, R.J.C. and Critchlow, G.W. (2009), "Effect of material, geometry, surface treatment and environment on the shear strength of single lap joints", *J. Adhes. Adhes.*, **29**(6), 621-632.

De'Nève, B., Delamar, M., Nguyen, T.T. and Shanahan, M.E.R. (1998), "Failure mode and ageing of steel/epoxy joints", *Appl. Surf. Sci.*, **134**(1-4), 202-212.

Elhannani, M., Madani, K., Legrand, E., Touzain, S. and Feaugas, X. (2017), "Numerical analysis of the effect of the presence, number and shape of bonding defect on the shear stresses distribution in an adhesive layer for the single-lap bonded joint; Part 1", *Aerosp. Sci. Technol.*, **62**, 122-135.

Elhannani, M., Madani, K., Mokhtari, M., Feaugas, X., Touzain, S. and Cohendoz, S. (2016), "A new analytical approach for optimization design of adhesively bonded single-lap joint", *Struct. Eng. Mech.*, **59**(2), 313-326.

Fu, M. and Mallick, P. (2001), "Fatigue of hybrid (adhesive/bolted) joints in SRIM composites", *J. Adhes. Adhes.*, **21**(2), 145-159.

Gomez, S., Onoro, J. and Pecharroman, J. (2007), "A simple mechanical model of a structural hybrid adhesive/riveted single lap joint", *J. Adhes. Adhes.*, **27**(4), 263-267.
Harris, J.A. and Adams, R.A. (1984), "Strength prediction of bonded single lap joints by nonlinear finite element methods", *J. Adhes. Adhes.*, **4**(2), 65-78.
Hart-Smith, L.J. (1973), "Adhesive-bonded double-lap joints", NASA-CR-112235; Douglas Aircraft Co., Inc., CA, U.S.A.
Hart-Smith, L.J. (1985), "Bonded-bolted composite joints", *J. Aircraft.*, **22**(11), 993-1000.
Ireman, T., Nyman, T. and Hellbom, K. (1993), "On design methods for bolted joints in composite aircraft structures", *Compos. Struct.*, **25**(1-4), 567-578.
Karachalios, E.F., Adams, R.D. and da Silva, L.F.M. (2013a), "Single lap joints loaded in tension with high strength steel adherends", *J. Adhes. Adhes.*, **43**, 81-95.
Karachalios, E.F., Adams, R.D. and da Silva, L.F.M. (2013b), "Single lap joints loaded intension with ductile steel adherends", *J. Adhes. Adhes.*, **43**, 96-108.
Kelly, G. (2006), "Quasi-static strength and fatigue life of hybrid (bonded/bolted) composite single-lap joints", *Compos. Struct.*, **72**(1), 119-129.
Kweon, J., Jung, J., Kim, T., Choi, J. and Kim, D. (2006), "Failure of carbon composite-to-aluminum joints with combined mechanical fastening and adhesive bonding", *Compos. Struct.*, **75**(1), 192-198.
Lee, M., Cho, T., Kim, W., Lee, B. and Lee, J. (2010), "Determination of cohesive parameters for a mixed-mode cohesive zone model", *J. Adhes. Adhes.*, **30**(5), 322-328.
Lee, M.H., Kim, H.Y., Oh, S.L. (2006), "Crushing test of double hat-shaped members of dissimilar materials with adhesively bonded and self-piercing riveted joining methods", *Thin-Walled Struct.*, **44**(4), 381-386.
Lees, W.A. (1985), "Stress distribution in bonded joints: an exploration within a mathematical model", *Mater. Des.*, **6**(3), 117–23.
Matthews, F.L., Kilty, P.F. and Goodwin, E.W. (1982), "A Review of the strength of joints in fibre reinforced plastics. Part 2 Adhesively bonded joints", *Compos.*, 29-37.
Mokhtari, M., Madani, K., Belhouari, M., Touzain, S., Feaugas, X. and Ratwani, M. (2013), "Effects of composite adherend properties on stresses in double lap bonded joints", *Mater. Design*, **44**, 633-639.
Peroni, L., Avalle, M. and Belingardi, G. (2009), "Comparison of the energy absorption capability of crash boxes assembled by spot-weld and continuous joining techniques", *J. Impact Eng.*, **36**(3), 498-511.
Reid, J.D. and Hiser, N.R. (2005), "Detailed modeling of bolted joints with slippage", *Finite Elem. Anal. Des.*, **41**(6), 547-562.
Rezgani, L., Madani, K. and Mokhtari, M., Feaugas, X., Cohendoz, S., Touzain, S. and Mallarino, S. (2018), "Hygrothermal ageing effect of ADEKIT A140 adhesive on the J-integral of a plate repaired by composite patch", *J. Adhes. Sci. Technol.*, **32**(13), 1393-1409.
Rezgani, L., Madani, K., Feaugas, X., Touzain, S. and Vallette, J. (2016), "Influence of water ingress onto the crack propagation rate in a AA2024-T3 plate repaired by a carbon/epoxy patch", *Aerosp. Sci. Technol.*, **55**, 359-365.
Russo, A. and Zuccarello, B. (2013), "Toward a design method for metal-composite co-cured joints based on the G-SIFs", *Compos. Part B: Eng.*, **45**(1), 631-643.
Sadowski, T., Kneć, M. and Golewski, P. (2010), "Experimental investigations and numerical modelling of steel adhesive joints reinforced by rivets", *J. Adhes. Adhes.*, **30**(5), 338-346.
Seo, D.W., Lim, J.K. (2005), "Tensile, bending and shears strength distributions of adhesive-bonded butt joint specimens", *Compos. Sci. Technol.*, **65**(9), 1421-1427.
Thrall, Jr. and Edward, W. (1977), "Primary adhesively bonded structure technology (PABST)", *J. Aircraft*, **14**(6), 588-594.
Thrall, Jr. and Edward, W. (1979), "PABST program test results", *Adhes.*, **22**(10), 22-33.
Tsai, M. and Morton, J. (1993), "Mechanics of a laminated composite single-lap joint", *Mechanics Composites Rev.*
Tsai, M. and Morton, J. (1995), "The effect of a spew fillet on adhesive stress distributions in laminated composite single-lap joints", *Compos. Struct.*, **32**(1-4), 123-131.
Tsai, M.Y. and Morton, J. (1994), "An evaluation of analytical and numerical solutions to the single-lap

joint", *Solids Struct*., **31**(18), 2537-2563.
Vinson, J.R. (1989), "Adhesive bonding of polymer composites", *Polym*. *Eng*. *Sci*., **29**(19), 1325-1331.
Völkersen, O. (1938), "Die Nietkraftverteilung in Zugbeanspruchten Neitverbeindun- gen mit Konstanten Laschequerschnitten", *Die Luftfahrtforschung*, **15**, 41-47.
Wooley, G.R. and Carver, D.R. (1971), "Stress concentration factors for bonded lap joints", *J*. *Aircraft*, **8**(10), 817-820.
Zhang, F., Wang, H.P., Hicks, C., Yang, X., Carlson, B. and Zhou, Q. (2013a), "Experimental study of initial strengths and hygro thermal degradation of adhesive joints between thin aluminum and steel substrates", *J*. *Adhes*. *Adhes*., **43**, 14-25.
Zhang, F., Yang, X., Wang, H.P., Zhang, X., Xia, Y. and Zhou, Q. (2013b), "Durability of adhesively- bonded single lap-shear joints in accelerated hygrothermal exposure for automotive applications", *J*. *Adhes*. *Adhes*., **44**, 130-137.

EC